Received: 10 October 2022 | Revised: 13 July 2023 | Accepted: 7 September 2023

DOI: 10.1111/gbi.12577

ORIGINAL ARTICLE

gebiology WILEY

# Divergence time estimates for the hypoxia-inducible factor-1 alpha (HIF1α) reveal an ancient emergence of animals in low-oxygen environments

Flavia A. Belato[1] | Beatriz Mello[2] | Christopher J. Coates[3] | Kenneth M. Halanych[4] | Federico D. Brown[1] | André C. Morandini[1] | Juliana de Moraes Leme[5] | Ricardo I. F. Trindade[6] | Elisa Maria Costa-Paiva[1,6]

[1]Institute of Biosciences, Department of Zoology, University of Sao Paulo, São Paulo – SP, Brazil

[2]Biology Institute, Genetics Department, Federal University of Rio de Janeiro, Rio de Janeiro – RJ, Brazil

[3]Zoology, Ryan Institute, School of Natural Sciences, University of Galway, Galway, Ireland

[4]Center for Marine Science, University of North Carolina Wilmington, Wilmington, North Carolina, USA

[5]Geoscience Institute, University of Sao Paulo, São Paulo – SP, Brazil

[6]Institute of Astronomy, Geophysics and Atmospheric Sciences, University of Sao Paulo, São Paulo – SP, Brazil

**Correspondence**
Elisa Maria Costa-Paiva, Institute of Biosciences, Department of Zoology, University of Sao Paulo, São Paulo – SP, Brazil.
Email: elisam.costapaiva@gmail.com

**Funding information**
Conselho Nacional de Desenvolvimento Científico e Tecnológico; Fundação de Amparo à Pesquisa do Estado de São Paulo; National Science Foundation

## Abstract

Unveiling the tempo and mode of animal evolution is necessary to understand the links between environmental changes and biological innovation. Although the earliest unambiguous metazoan fossils date to the late Ediacaran period, molecular clock estimates agree that the last common ancestor (LCA) of all extant animals emerged ~850 Ma, in the Tonian period, before the oldest evidence for widespread ocean oxygenation at ~635–560 Ma in the Ediacaran period. Metazoans are aerobic organisms, that is, they are dependent on oxygen to survive. In low-oxygen conditions, most animals have an evolutionarily conserved pathway for maintaining oxygen homeostasis that triggers physiological changes in gene expression via the hypoxia-inducible factor (HIFa). However, here we confirm the absence of the characteristic HIFa protein domain responsible for the oxygen sensing of HIFa in sponges and ctenophores, indicating the LCA of metazoans lacked the functional protein domain as well, and so could have maintained their transcription levels unaltered under the very low-oxygen concentrations of their environments. Using Bayesian relaxed molecular clock dating, we inferred that the ancestral gene lineage responsible for HIFa arose in the Mesoproterozoic Era, ~1273 Ma (Credibility Interval 957–1621 Ma), consistent with the idea that important genetic machinery associated with animals evolved much earlier than the LCA of animals. Our data suggest at least two duplication events in the evolutionary history of HIFa, which generated three vertebrate paralogs, products of the two successive whole-genome duplications that occurred in the vertebrate LCA. Overall, our results support the hypothesis of a pre-Tonian emergence of metazoans under low-oxygen conditions, and an increase in oxygen response elements during animal evolution.

## 1 | INTRODUCTION

Defining when metazoans first emerged is crucial to understanding the processes of early animal life. Although pre-Cambrian fossil records of animals remain scarce and controversial (e.g., debated organic biomarkers of sponges from the Cryogenian period (>635 Ma) and Tonian period, >890 Ma (Antcliffe et al., 2014; Brain et al., 2012; Love et al., 2009; Turner, 2021; Yin et al., 2015). The currently accepted earliest fossil record of an undisputed animal is from the late Ediacaran period ~571 Ma (Droser et al., 2017;

  

Narbonne, 2005; Pu et al., 2016; Wood et al., 2019). In contrast, most molecular clock estimates agree that the last common ancestor of all extant animals emerged ~850 Ma in the Tonian period, before the onset of long-term global glaciations (~720–635 Ma) (Cunningham et al., 2017; Dohrmann & Wörheide, 2017; dos Reis et al., 2015; Erwin et al., 2011). Estimates for the timing of animal diversification, using different calibration points and molecular datasets, range from 1298 to 615 Ma (Cartwright & Collins, 2007; Dohrmann & Wörheide, 2017; dos Reis et al., 2015; Douzery et al., 2004; Erwin et al., 2011; Hedges et al., 2004; Parfrey et al., 2011; Peterson et al., 2004). Nevertheless, almost all these molecular estimates place the emergence of animals long before the oldest evidence for ocean oxygenation pulses at ~635–560 Ma in the Ediacaran period (Lenton & Daines, 2017; Sahoo et al., 2012; Tostevin & Mills, 2020; Wood et al., 2019; Zhang et al., 2018).

As strictly aerobic organisms, metazoans are dependent on oxygen as the main electron acceptor during oxidative metabolism for energy production (Kaelin & Ratcliffe, 2008; Semenza, 2007). Recent studies on the geochemistry of the ancient Earth suggest that Cryogenian to Ediacaran oceans had no more than 1–10% of modern atmospheric oxygen saturation (Lenton, 2020; Lenton & Daines, 2017; Liu et al., 2021; Lyons et al., 2014; Mills et al., 2022), environmental low-oxygen levels could have limited metazoans by placing energetic constraints on the diversity, abundance, and physiology of early animals (Cole et al., 2020; Fenchel & Finlay, 1995; Reinhard et al., 2016). When exposed to hypoxia, most animals have an evolutionarily conserved pathway for maintaining physiological oxygen homeostasis that triggers adaptive changes in gene expression. This pathway is mediated by the transcription factor hypoxia-inducible factor 1 (HIF-1) (Kaelin & Ratcliffe, 2008; Loenarz et al., 2011; Semenza, 2007). HIF1 consists of two subunits: an oxygen-regulated HIF1a and a constitutively expressed HIF1b (Aryl Hydrocarbon Receptor Nuclear Translocator, ARNT). Both subunits are composed of two basic helix–loop–helix (bHLH) and Per-ARNT-Sim (PAS) domains that allow subunit dimerization when cellular oxygen concentrations are low. They promote the transcription of hundreds of genes involved in mitochondrial function, energy metabolism, oxygen binding and delivery, and hematopoiesis (Kaelin & Ratcliffe, 2008; Semenza, 2007). HIFa is continuously synthesized and degraded when oxygen supply is sufficient (normoxia; Figure 1). Prolyl hydroxylases (PHD) target defined proline residues (called the oxygen-dependent degradation domain, ODDD, on the HIF1a subunit (Figure 2a; Hon et al., 2002), which are recognized by the von Hippel–Lindau (VHL) protein and promote the ubiquitination mediated proteasomal degradation of HIF1a (Kaelin & Ratcliffe, 2008; Min et al., 2002; Semenza, 2007). Another hydroxylase, FIH1 (factor inhibiting HIF1), prevents the transcriptional activity of any HIF1a that has not been degraded (Kaelin & Ratcliffe, 2008; Peet & Linke, 2006; Semenza, 2007). During hypoxia, PHD and FIH1 are inactivated, and therefore, HIF1a is protected from degradation, accumulates within the cell, and dimerizes with HIF1b forming a heterodimeric HIF1a/HIF1b complex (Semenza, 2007). The complex translocates to the nucleus and upregulates genes associated with oxygen conservation (Figure 1; Semenza, 2007; Kaelin & Ratcliffe, 2008).

Although all animals need oxygen to survive, their demands are not the same. Sponges and ctenophores, which are likely sister groups to all remaining animal phyla (Halanych, 2016; King & Rokas, 2017; Pisani et al., 2015; Whelan et al., 2015), can live under low-oxygen concentrations (Levin, 2003; Mosch et al., 2012; Purcell et al., 2001; Thuesen et al., 2005). Experimental outcomes demonstrated that

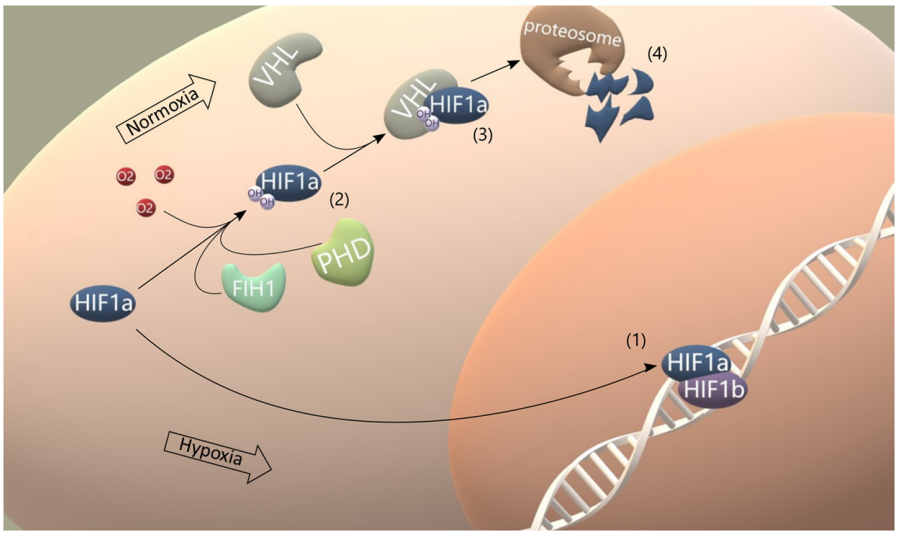


**FIGURE 1** Hypoxia-inducible factor pathway. When oxygen levels are sufficient oxygen is available (normoxia), HIF1a subunit is continuously synthesized and degraded. Two hydroxylases, prolyl hydroxylases (PHD) and factor inhibiting HIF1 (FIH1), hydroxylate the HIF1a subunit (2). The von Hippel–Lindau (VHL) protein recognizes the hydroxyls (3) and promotes the ubiquitination and immediate degradation of HIF1a via the proteasome (4). These processes are inhibited when oxygen is low (hypoxia) due to hydroxylase inactivation leading to a rapid stabilization of HIF1a, which is protected from degradation, accumulates within the cytoplasm, binds to HIF1b (1), forms the transcriptionally active HIF heterodimer, and enters the nucleus.

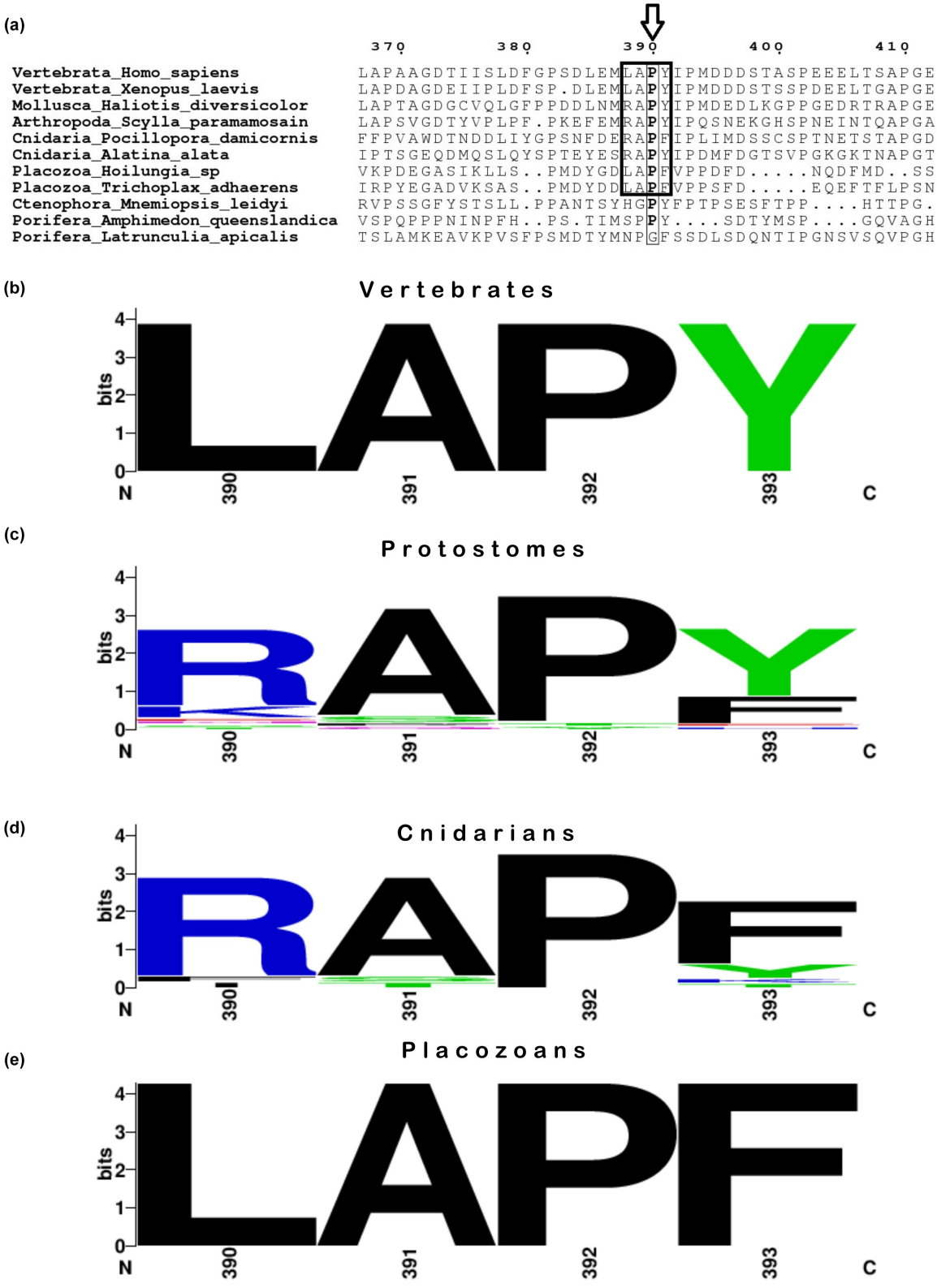


FIGURE 2 Characteristic HIFa domain in metazoans. (a) Multiple amino acid sequence alignment of positions surrounding the HIFa oxygen-dependent degradation domain (ODDD) in metazoans. The domain is indicated by the black bold box. Invariant amino acid residues are marked in bold. We do not find the ODDD motif in any sponge or ctenophore sequences. (b) Sequence logo of the position weight matrix of the ODDD from our 35 vertebrate sequences. (c) Sequence logo of the position weight matrix of the ODDD from our 47 protostome sequences. (d) Sequence logo of the position weight matrix of the ODDD from our 18 cnidarian sequences. (e) Sequence logo of the position weight matrix of the ODDD from our two placozoan sequences. Sequence logos were obtained using WebLogo (Crooks et al., 2004).

these early-diverging clades lack key components of the HIF pathway, implying they have very low-oxygen requirements (Mills et al., 2014; Mills, Francis, Vargas, et al., 2018). The last common ancestor of metazoans may also have lacked a functional HIF pathway and maintained aerobic metabolism and normal transcription in oxygen-poor environments (Mills, Francis, Vargas, et al., 2018). In support of this hypothesis, recent works have proposed that early animals were likely small, soft-bodied, collagen-poor, and restricted their use of oxygen to high-priority physiological functions (Cole et al., 2020; Mills et al., 2014).

Molecular dating techniques, which consist of estimating the age of internal nodes of a phylogenetic tree based on molecular sequences using mainly fossil calibrations (Ho & Duchêne, 2014; Mello, 2018), have advanced tremendously in recent years. They are now considered standard methods to infer dates of divergence essential to elucidating evolutionary processes that led to the diversification of major taxa through Earth's geological history (Delsuc et al., 2018; dos Reis et al., 2015; Ho & Duchêne, 2014; Irisarri et al., 2017; Misof et al., 2014; Wolfe et al., 2019). Divergence time estimates are applied to gene trees to infer the origin of various physiological modalities. Consequently, our understanding of the tempo and mode of early animal evolution can be enhanced by molecular dating of specific genes and proteins (Shih & Matzke, 2013; Yu & Li, 2014; Bezerra et al., 2021; Boden et al., 2021; Costa-Paiva et al., 2021).

Herein, we explored divergence estimates for HIFa genes to elucidate their evolutionary history. Oxygen is crucial for all animals, as such, investigating the evolutionary history of a protein involved crucially in oxygen homeostasis, namely HIFa (Semenza, 2007), provides an effective source of knowledge on the emergence and diversification of animals. By applying a Bayesian uncorrelated relaxed clock to a HIFa dataset with representative sampling of all major animal lineages, our data support a pre-Tonian emergence of the ancestral gene lineage that later originated metazoan HIFa, consistent with previous molecular clock estimates for an ancient origin of animals (Dohrmann & Wörheide, 2017).

## 2 | METHODS

### 2.1 | Data acquisition

Sequences were obtained from three different sources: 1) WormNet II transcriptomes generated by our research group, 2) NCBI database, and 3) Mills, Francis, Vargas, et al. (2018) and Graham and Presnell (2017) (all listed in File S1). First, we used the transcriptomes of 77 metazoan species collected as part of the WormNet II project on annelid phylogeny (Weigert et al., 2014). Specimens were collected by several techniques, including intertidal sampling, dredging and box cores, and preserved either in RNALater or frozen at −80°C. RNA extraction, cDNA library preparation, and high-throughput sequencing protocols followed Kocot et al. (2011) and Whelan et al. (2015). Subsequently, total RNA was extracted using TRIzol (Invitrogen) either from whole animals or from the body walls and purified with on-column DNase digestion of the RNeasy kit (Qiagen). The SMART cDNA Library Construction Kit (Clontech) was used to reverse transcribe the single-stranded RNA templates. The Advantage 2 PCR system (Clontech) was used to synthesize double-stranded cDNA. Barcoding and library sequencing were performed with Illumina technology by The Genomic Services Lab at the Hudson Alpha Institute. Because transcriptomic sequencing was carried out from 2012 to 2015, paired-end runs were of 100 or 125 bp in length, using either v3 or v4 chemistry on Illumina HiSeq 2000 or 2500 platforms. Finally, to facilitate sequence assembly, paired-end transcriptome data were digitally normalized to an average k-mer coverage of 30 using the script normalize-by-median.py (Brown et al., 2012). Transcriptomes were assembled using Trinity r2013-02-25 with default settings (Grabherr et al., 2011).

All transcriptomes were annotated using the Trinotate annotation pipeline (http://trinotate.github.io/) (Grabherr et al., 2011). This pipeline uses a BLAST-based method against the EggNOG 4.5.1 v (Huerta-Cepas et al., 2016) and KEGG (Kanehisa et al., 2012) databases to provide the gene ontology annotations. Gene ontology is a standardized functional classification system for genes that describe properties of genes and their products using a dynamic-updated controlled vocabulary (Gene Ontology Consortium, 2004). Software used with the Trinotate pipeline included HMMER 3.2.1 for protein domain identification (Finn et al., 2011); tmHMM 2.0 for prediction of transmembrane helices of proteins (Krogh et al., 2001); RNAmmer 1.2 for prediction of ribosomal RNA (Lagesen et al., 2007); SignalP 4.1 to predict signal peptide cleavage sites (Petersen et al., 2011); GOseq for prediction of the gene ontology (Young et al., 2010); EggNOG 4.5.1 for searching orthologous groups of genes (Huerta-Cepas et al., 2016).

After Trinotate annotation, retrieved transcriptome sequences were verified to select sequences functionally assigned as hypoxia-inducible factor 1-alpha (HIF1a) genes. Sequences identified as HIF1a genes were translated from RNA into amino acids using TransDecoder with default settings (https://transdecoder.github.io/). TransDecoder translation can produce multiple open reading frames (ORFs); therefore, the homology between sequences was confirmed based on structural motif presence, validating the Pfam domain (Finn et al., 2016) of translated protein sequences against the EMBL-EBI protein database with an e-value cutoff of $10^{-5}$. Sequences with a minimum length of 300 amino acid residues with a verified bHLH-PAS domain were retained for further analysis. Because HIF genes are part of the larger bHLH-PAS protein family, we only selected sequences that contained this domain.

Our second source of HIF1a sequences was the National Center for Biotechnology Information (NCBI) database. We searched for protein sequences functionally annotated as hypoxia-inducible factor 1-alpha on GenBank, focusing mainly on invertebrate sequences. "Putative," "Hypothetical," "Low-quality," and "partial" sequences were excluded, as well as those with fewer than 300 amino acids. Pfam domain validation (Finn et al., 2016) with an e-value cutoff of $10^{-5}$ was performed and the presence of the bHLH-PAS domain was verified. To expand our dataset, we obtained 89 HIFa sequences from different metazoans, including vertebrates, from Mills, Francis,

Vargas, et al. (2018) using their HIFa project dataset (https://bitbucket.org/molpalmuc/sponge-oxygen/src/master/) and Graham and Presnell (2017) (https://doi.org/10.1371/journal.pone.0179545.s001). All sequence information is detailed in File S1.

## 2.2 | Alignments and phylogenetic reconstructions

Sequences ($n = 218$) were aligned in MAFFT using the E-INS-I algorithm (Katoh & Standley, 2013), and gap-rich regions were removed in trimAl 1.2 (Capella-Gutierrez et al., 2009) using a gap threshold of 0.75. To remove spuriously aligned sequences based on similarity to the alignment, sequences were manually inspected with Geneious 11.1.2 (Kearse et al., 2012). To eliminate dataset redundancy, identical sequences were removed. The resulting amino acid alignment of 136 sequences was analyzed further.

Statistical selection of the best-fit model of protein evolution was carried out using the Akaike and Bayesian Information Criteria (AIC and BIC, respectively; Darriba et al., 2011) with ModelFinder in IQ-Tree software (Kalyaanamoorthy et al., 2017). Two different phylogenetic inference methods were employed in our analysis: (1) a maximum likelihood routine in IQ-Tree (Nguyen et al., 2015) with 1000 ultrafast bootstrap replicates (UFBoot; Minh et al., 2013); (2) Bayesian inference using MrBayes 3.2.7 (Ronquist & Huelsenbeck, 2003) with two independent runs, each containing four Metropolis-coupled chains of $10^7$ generations that were sampled every 500th generation to approximate posterior distributions. To confirm whether chains achieved stationarity and to determine an appropriate burn-in, we evaluated trace plots of all MrBayes parameter outputs in Tracer v1.6 (Rambaut et al., 2015). The first 25% of samples were discarded as burn-in and a majority rule consensus tree was generated using MrBayes. Bayesian posterior probabilities were used to gauge the statistical support of each bipartition. Because of the evolutionary time depth of our dataset, phylogenetic reconstruction was also performed with a mixture model in IQ-Tree to help alleviate the issues related to saturation and long-branch attraction by accommodating site-specific features of protein evolution (Lartillot et al., 2007; Lartillot & Philippe, 2004). To consider heterogeneity at the site level in the Bayesian reconstruction, we ran an analysis in PhyloBayes (Lartillot et al., 2009) using the CAT-GTR mixture model. The program was run twice to check for convergence of the chains, which was accessed by the maxdiff value (maxdiff was <0.1). Trees were visualized in FigTree 1.4.3 (Rambaut, 2009) and rooted using two bHLH-PAS protein sequences of the single-celled eukaryotic outgroup, *Capsaspora owczarzaki* (Mills, Francis, Vargas, et al., 2018; Suga et al., 2013).

## 2.3 | Molecular dating

BEAST 2.4.7 (Bouckaert et al., 2014) was used to obtain divergence time estimates with an uncorrelated lognormal relaxed clock (Drummond et al., 2006), the LG substitution model (Whelan & Goldman, 2001) and a birth–death tree prior with default settings. As calibration information derived from fossil data provides information regarding the split times between biological lineages (i.e., speciation events), only speciation nodes were considered to calibrate divergence times. Therefore, divergences classified as speciation nodes that reflected robust biological clades and were free of duplication events were chosen. These were the LCA of seven crown nodes: Vertebrata, Actinopterygii, Sarcopterygii (including Tetrapoda), Ambulacraria, Mollusca, Pancrustacea, and Cnidaria. For Actinopterygii and Sarcopterygii, the requirements cited above were met three times (i.e., speciation nodes that included only Actinopterygii or Sarcopterygii HIFa sequences were recovered three times each in the estimated phylogeny). Therefore, 11 speciation nodes were calibrated with uniform distributions with lower and upper boundaries based on calibration information from Benton et al. (2015) and dos Reis et al. (2015).

The date range (minimum and maximum boundaries of the uniform distributions) used to calibrate the time of the Most Recent Common Ancestor (tMRCA) for Vertebrata was 457.5–636.1 Ma, Actinopterygii was 378.19–422.4 Ma, Sarcopterygii was 408–427.9 Ma, Ambulacraria was 515.5–636.1 Ma, Mollusca was 534–549 Ma, Pancrustacea was 514–531.22 Ma, and Cnidaria was 529–636.1 Ma. All calibration points were obtained from dos Reis et al. (2015) and Benton et al. (2015) using coherent criteria accordingly with Parham et al. (2012). Notably, calibrated nodes were constrained to be monophyletic, while other phylogenetic relationships were estimated in BEAST. Markov Chain Monte Carlo (MCMC) was run for 200 million generations with a sampling frequency of 10,000 and a discarded burn-in period of 20 million generations (10%). To access the convergence of chains, two independent MCMC runs were performed. In both runs, after discarding the burn-in period, effective sample sizes (ESS) values were higher than 200. The resulting timetree was plotted using the "geoscalePhylo" function ("strap" R v.4.0.3 package; Bell & Lloyd, 2015) and modified using Inkscape v1.1.1.

To verify the robustness of the divergence times estimates generated in BEAST, we performed molecular dating analyses using different parameters in MCMCTree (Yang, 2007). MCMCTree analyses were performed using the fixed topologies obtained in BEAST and IQ-Tree. We considered independent and correlated evolutionary rates, and an additional calibration at the root, which was a soft maximum of 833 Ma, based on dos Reis et al. (2015) and Benton et al. (2015). All MCMCTree analyses were conducted under the approximate likelihood calculation method (dos Reis and dos Reis & Yang, 2011), with at least two chains to check for convergence.

# 3 | RESULTS

The final dataset consisted of 134 HIFa sequences (File S1) from 115 metazoan species and two bHLH-PAS sequences (outgroup) from

the unicellular eukaryotic filozoan *Capsaspora owczarzaki* (Mills, Francis, Vargas, et al., 2018; Suga et al., 2013). After alignments and trimming, the final alignment had a maximum sequence length of 416 amino acids (File S2, and https://figshare.com/s/54350fa8b7573951990b). Untrimmed sequences are available in File S3 and at https://figshare.com/s/f14d22a30cb636d0bd93. The 33 sequences obtained from the WormNet II database were deposited at GenBank under accessions OQ354979–OQ355011. The best fitting standard substitution model for both Bayesian and maximum likelihood analyses according to ModelFinder was WAG (Whelan & Goldman, 2001). The best maximum likelihood mixture model was LG+C40+F+G. Phylogenetic reconstructions performed with mixture models (IQ-Tree mixture model tree file available at https://figshare.com/s/0369cceffa0947d93ca8 and PhyloBayes mixture model tree file available at https://figshare.com/s/a6b98a40d0949dc60750) were in agreement with Bayesian and maximum likelihood phylogenies based on site-homogeneous substitution models (Files S4 and S5). All datasets, alignments, and tree files used in this work are publicly available at https://figshare.com/projects/Divergence_time_estimates_for_the_hypoxia-inducible_factor-1_alpha_HIF1_reveal_an_ancient_emergence_of_animals_in_low-oxygen_environments/164017.

All HIFa proteins have a characteristic motif with a key proline residue (preceded by an alanine) that signals the protein for degradation, this region is called the oxygen-dependent degradation domain (ODDD) (Figure 2a; Tarade et al., 2019). The motif varies between clades, where the LAPY motif in vertebrate HIFa is instead RAPY in most protostomes, RAPY or RAPF in cnidarians, and LAPF in placozoans (Figure 2b–e). None of these motifs were found in the five sponge and single ctenophore homolog sequences retrieved from the transcriptomes we queried.

Bayesian and maximum likelihood inferences generated similar tree topologies with several strongly supported clades (Figure 3; Files S4 and S5). The main difference was the Bayesian tree presented some poorly resolved nodes in Arthropoda and Mollusca (File S4), whereas the maximum likelihood inference recovered strongly supported nodes in those clades. The position of both sponges and ctenophore in the tree suggests that sequences of sponges and ctenophore are sisters to all HIFa proteins (Figure 3). Although all metazoan sequences formed a monophyletic group, the absence of the characteristic HIFa domain in the five sponge and single ctenophore sequences suggests they are not true HIFa due to the absence of an ODDD motif, as previously suggested by Mills, Francis, Vargas, et al. (2018).

HIFa sequences that clustered into monophyletic groups, representing recognized phyla, with strong statistical support were the placozoans (100%; PP=1; clade XII; Figure 3), cnidarians (100%; PP=1; clade XI; Figure 3), arthropods (93%; clade X; Figure 3), phoronids (100%; PP=1; clade IX; Figure 3), brachiopods (86%; clade VIII; Figure 3), mollusks (96%; clade VII; Figure 3), hemichordates (87%; PP=1; clade VI; Figure 3), echinoderms (100%; PP=1; clade V; Figure 3), and cephalochordates (100%; PP=1; clade IV; Figure 3). A single nemertine sequence fell within annelids rendering Annelida non-monophyletic (Figure 3). Notably, the *Ciona intestinalis* sequence fell in an odd position within the tree (Figure 3). However, we chose to maintain this sequence because other works analyzed it and yielded similarly unusual results (Graham & Presnell, 2017; Mills, Francis, Vargas, et al., 2018). We considered the position of *C. intestinalis* as an artifact that needs further investigation (Figure 3). Importantly, tunicate sequences have high rates of substitution (Berná & Alvarez-Valin, 2014; Tsagkogeorga et al., 2009, 2012).

According to our gene genealogy obtained for the HIFa family, vertebrate HIFa arose from a series of duplication events that brought about three distinct vertebrate HIFa clades: HIF1a, HIF2a, and HIF3a (Clades I, 100%; PP=1; II, 100%; PP=1; III, 100%; PP=1; Figure 3). Up to five HIFa protein sequences were identified in vertebrate specimens (e.g., zebrafish *Danio rerio*), and these paralogs most likely resulted from multiple genome duplication events that occurred in the vertebrate stem lineage, and signatures of the two rounds of vertebrate genome duplication can be clearly seen in the HIFa gene tree (arrows and asterisks, Figure 3). Additional paralogs seen in *D. rerio* were most likely a result of the teleost-specific whole-genome duplication (Glasauer & Neuhauss, 2014).

The tree topology estimated by BEAST was mostly congruent with those obtained by IQ-Tree and MrBayes (Figure 4, tree file available at https://figshare.com/s/72173e8c3b390ac9c55a). The posterior distributions of estimated node ages were wide, probably due to the short alignment length. Therefore, all the estimated times are reported along with their credibility intervals (CrIs). The estimated age for the LCA gene that later gave rise to the gene lineage including metazoan HIFa genes, sponge homologs, and ctenophore homologs was ~1273 Ma (Credibility Interval (CrI) 957–1621 Ma) in the Mesoproterozoic (Figure 4). Cnidarian and placozoan HIFa sequences diverged from sponges and ctenophores homologs at 1218 Ma (CrI 760–1331 Ma). The bilaterian HIFa lineage originated at 959 Ma (CrI 801–1122 Ma) in the Neoproterozoic Era (Figure 4). The estimated time of the emergence of cnidarian HIFa was 594 Ma (CrI 541–636 Ma) in the Ediacaran Period. The divergence time estimated for the appearance of arthropodan HIFa occurred at 651 Ma (CrI 522–788 Ma) in the Cryogenian Period, with mollusk HIFa emerging at 541 Ma (CrI 534–548 Ma) in the Ediacaran Period. The deuterostome HIFa lineage originated at 748 Ma (CrI 652–842 Ma) in the Cryogenian Period. Two duplication events occurred in the vertebrate HIFa lineage (gray circles, Figure 4), both in the Ediacaran Period. The first event gave rise to vertebrate HIF2a and the lineage that would originate HIF1a+HIF3a occurred at 595 Ma (CrI 550–636 Ma). Subsequently, the second duplication event at 558 Ma (CrI 500–604 Ma) led to the appearance of vertebrate HIF1a and HIF3a.

Divergence time estimates obtained in MCMCTree using distinct fixed topologies (from BEAST and IQ-Tree), substitution rate models and the inclusion of a soft maximum calibration at the tree root showed high congruence with those obtained originally in BEAST (File S6). Divergence dates inferred for relevant nodes such as the root, the divergence of sponge and ctenophore homologs from all other animals, and the gene duplication events in vertebrates were mostly congruent among all analyses. Estimates obtained with

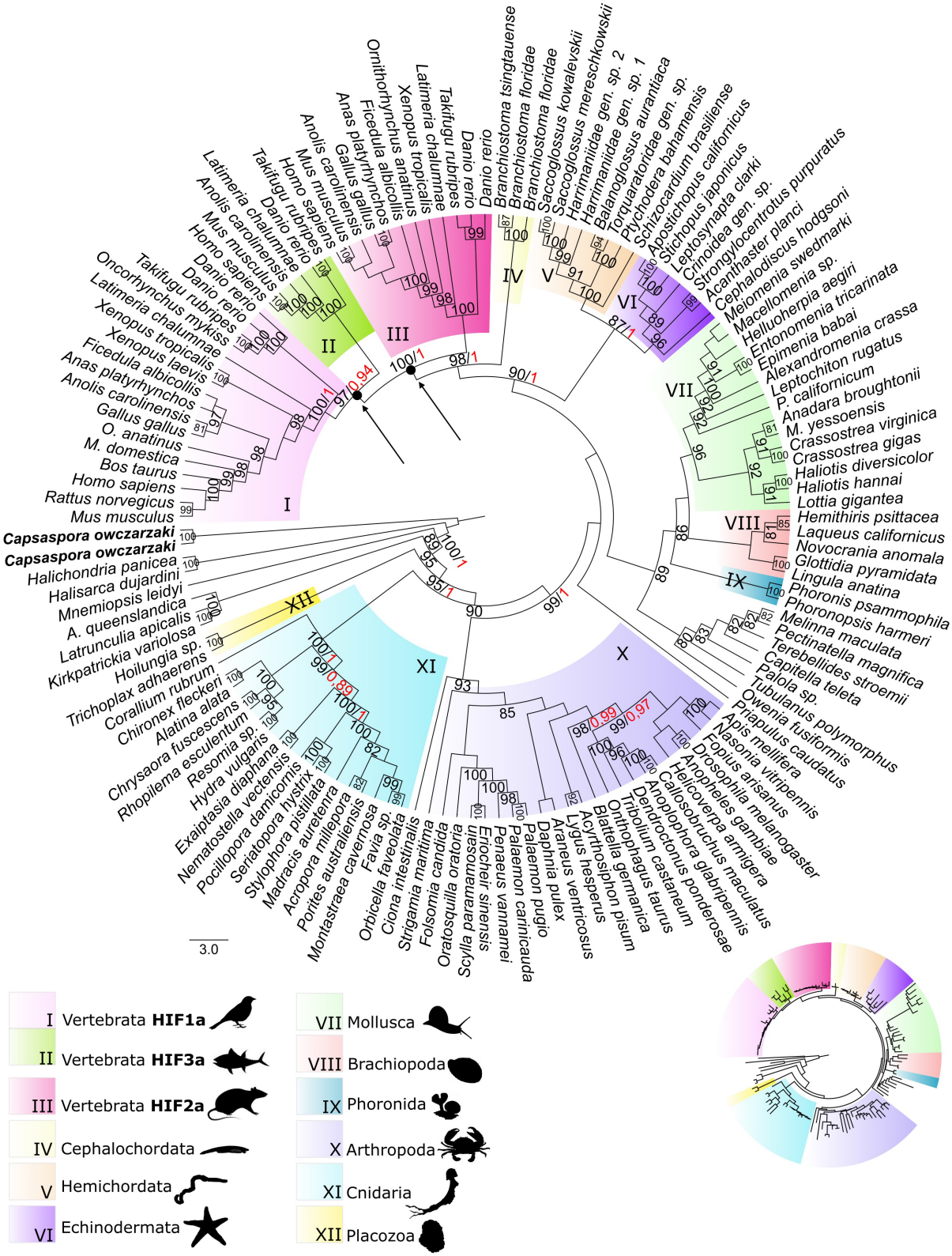


FIGURE 3 HIFa gene tree rooted with two capsasporan bHLH-PAS protein sequences. Clade I contains vertebrate HIF1a sequences. Clade II is composed of vertebrate HIF3a sequences. Clade III is formed by vertebrate HIF2a sequences. Clade IV represents cephalochordate HIFa genes. Clade V is composed of hemichordate HIFa sequences. Clade VI contains echinoderm HIFa genes. Clade VII represents mollusk HIFa sequences. Clade VIII is formed by brachiopods HIFa sequences. Clade IX contains phoronids HIFa genes. Clade X represents arthropods HIFa genes. Clade XI is composed of cnidarian HIFa genes. Clade XII represents placozoan HIFa genes. Black arrows and dots indicate gene duplication events. Bootstrap support values (in black) obtained from the maximum likelihood and the Bayesian posterior probabilities values (in red) shown (BP/PP). Support values >80 or 0.8 are shown. Sequences in bold represent the two capsasporan bHLH-PAS proteins used to root the tree. Inset; small topology showing branch lengths with the same color scheme.

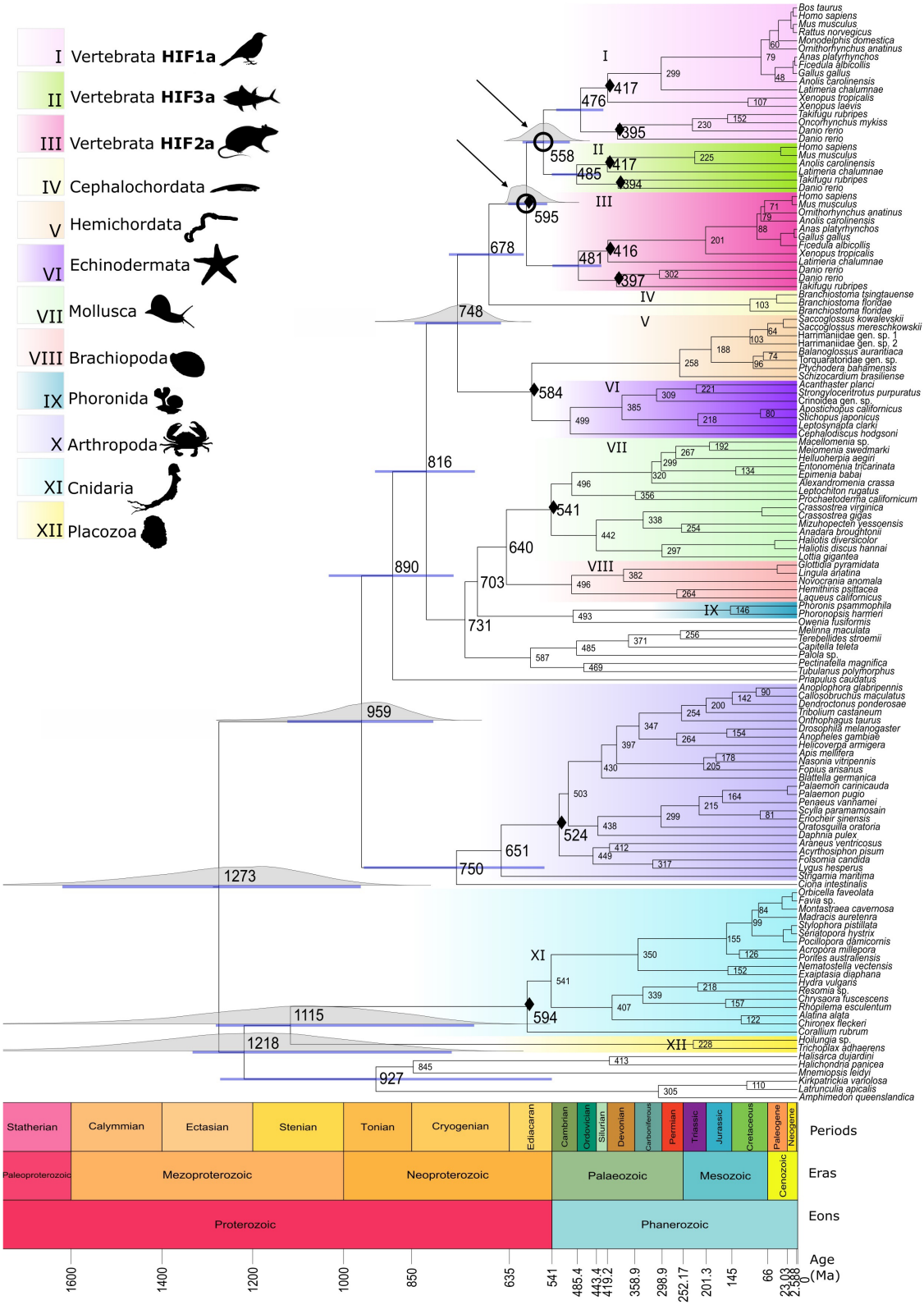


**FIGURE 4** Timetree of the HIFa genes. Clade I contains vertebrate HIF1a sequences; Clade II is vertebrate HIF3a sequences; Clade III is vertebrate HIF2a sequences; Clade IV represents cephalochordate HIFa sequences; Clade V is hemichordate HIFa sequences; Clade VI is echinoderm HIFa genes; Clade VII represents mollusk HIFa sequences; Clade VIII is brachiopods HIFa sequences; Clade IX contains phoronids HIFa sequences; Clade X represent arthropod HIFa; Clade XI is cnidarian HIFa sequences; Clade XII represents placozoan HIFa; Black arrows and circles indicate gene duplication events. Black diamonds indicate calibration nodes. Node ages are plotted, blue node bars are displaying 95% CrI and above them density plots highlighting the posterior distribution of node age estimates are shown for key nodes.

MCMCTree validated those retrieved by BEAST, which demonstrates the consistency of our results (regardless of the selected models).

## 4 | DISCUSSION

Our results demonstrate the ancestral gene lineage that originated the metazoan HIFa emerged at approximately 1273 Ma (CrI 957–1621 Ma) in the Mesoproterozoic Era (Figure 4), earlier than the dawn of metazoans. Additionally, we unveiled two duplication events in the evolutionary history of HIFa, ~595 Ma (CrI 550–636 Ma) and ~558 Ma (CrI 500–604 Ma) (Figure 4), generating three vertebrate HIFa paralogs. Although a functional HIFa appeared after the split of all other animals from sponges and ctenophores (Mills, Francis, Vargas, et al., 2018), as corroborated by our results, the molecular toolkit of HIFa was most likely present in metazoan ancestors. An important fraction of the molecular genetic toolkit required for animal development evolved much earlier in their eukaryotic unicellular ancestors (de Mendoza et al., 2013; Sebé-Pedrós et al., 2011, 2012). In fact, homologs of bHLH-PAS proteins were already present in the LCA of *Capsaspora*, choanoflagellates, and metazoans (Opisthokonta) between 1389 and 1240 Ma (Degnan et al., 2009; Parfrey et al., 2011; Sebé-Pedrós et al., 2011, 2012; Simionato et al., 2007), which complements with our results. During metazoan evolution, bHLH-PAS proteins were cooptated, resulting in new cellular pathways and function (Kaelin & Ratcliffe, 2008; Rodriguez-Pascual & Slatter, 2016; Rytkönen et al., 2011; Sebé-Pedrós et al., 2011).

A functional HIFa emerged most likely in the Mesoproterozoic Era, as showed by both BEAST (Figure 4) and MCMCTree divergence estimates (node 8 in File S6). HIFa proteins have their availability and therefore activity regulated by oxygen variation within the cells (Kaelin & Ratcliffe, 2008; Min et al., 2002; Semenza, 2007). They are sensitive to oxygen due to their unique oxygen-dependent degradation domain (ODDD), which has a key proline residue (preceded by an alanine) that signals the HIFa protein for degradation in the presence of oxygen (Figure 2a; Hon et al., 2002; Tarade et al., 2019). We did not find the characteristic HIFa motif (ODDD) in ctenophore and sponge sequences, which corroborate the reports of Mills, Francis, Vargas, et al. (2018) who suggest the organisms are not expected to respond to oxygen availability, and therefore, HIFa protein absence is expected.

Although atmospheric oxygen accumulated during the Great Oxidation Event (2.5–2.3 billion years ago (Ga; Kump, 2008), it remained at low levels throughout the Paleoproterozoic and Mesoproterozoic Eras (2.5–1.0 Ga; Farquhar et al., 2000). Before rising to modern oxygen levels in the Neoproterozoic (1.0–0.54 Ga; Och & Shields-Zhou, 2012). Recent proxy records of atmospheric oxygen and marine redox states suggest dynamic pulses of oxygenation against a background of gradually rising oxygen levels through this Era (Neoproterozoic Oxygenation Windows—NOW; Wood et al., 2019; Tostevin & Mills, 2020), instead of a single oxygenation event as proposed before (Canfield et al., 2007; Sperling et al., 2015). These events generated oxygen concentration levels that facilitated the metabolic needs of larger, more complex animals (Canfield et al., 2007). Larger-bodied animals have higher oxygen demands, but interestingly, regions of the body where embryonic and progenitor cells occur are generally hypoxic (Hammarlund et al., 2018; Nakamura et al., 2021). To meet the energetic and structural demands of larger animals, oxygen is necessary to maintain ATP production through the mitochondrial respiratory chain, and to synthesize collagen (Mills & Canfield, 2014; Semenza, 2007; Sperling et al., 2013). Hypoxic periods in animal evolution—generated by changes in the carbon cycle and oceanic redox conditions of the Cryogenian–Cambrian interval (Canfield & Farquhar, 2009; Lenton & Daines, 2017, 2018; Li et al., 2015)—may have resulted in driven distinct adaptations to regulate aerobic metabolism, which is consistent with the emergence of a bilaterian HIFa ca. 959 Ma (CrI 801–1122 Ma) in the Neoproterozoic Era (Figure 4).

Atmospheric oxygen levels may have provided a selection force on the development of cellular oxygen-sensing pathways (Mills, Francis, Vargas, et al., 2018; Taylor & McElwain, 2010). Hypoxia influences gene expression, the level of epigenetic modifications in cells, and is considered to play an essential role in early embryo development, cell differentiation, stem cell renewal, and cellular reprogramming (Alderman et al., 2019; Dunwoodie, 2009; Nakamura et al., 2021; Song et al., 2021; Tsuji et al., 2014; Wang et al., 2016). In plants and animals, low levels of oxygen are required to maintain the undifferentiated state of cells and influence their proliferation and cell fate (Nakamura et al., 2021; Simon & Keith, 2008; Weits et al., 2019), therefore, HIFa is hypothesized as essential for the evolution, and control of stem cells during the origin and evolution of metazoans (Hammarlund, 2020; Hammarlund et al., 2018). Although all metazoans—except Ctenophora and Porifera—express HIF1a, PHD, and VHL (Tarade et al., 2019), the presence of stem cells in low-oxygen environments in the bodies of marine invertebrates is largely undocumented. Investigating whether these animal cell types have retained a symplesiomorphic state of early primordial metazoan cell types, which presumably evolved a capacity to replicate and differentiate into cells that are more complex during hypoxic periods of the Neoproterozoic, would be the next step to advance this topic (Hammarlund et al., 2018; Mills, Francis, & Canfield, 2018; Nakamura et al., 2021). Sponge, cnidarian, and other marine invertebrate can de-differentiate or trans-differentiate (Adamska, 2018; Ferrario et al., 2020; Gold & Jacobs, 2013); therefore, it has been hypothesized that hypoxia and HIFa are involved in the fine-tuning of stem cell plasticity and development (Hammarlund, 2020).

Up to three HIFa proteins were identified in vertebrates, with *D. rerio* having five HIFa genes (File S1, Figure 3). Herein, the gene genealogy of HIFa (Figures 3 and 4) supports the existence of three HIF paralogs in extant vertebrates that are most likely products of the two successive whole-genome duplications (WGD) events from 700 to 450 Ma in the LCA of vertebrates (Kuraku et al., 2008; Panopoulou & Poustka, 2005; Sacerdot et al., 2018; Simakov et al., 2020). Estimated ages for the duplication events that originated the three vertebrate paralogs, ~595 Ma (CrI 550–636 Ma) and ~558 Ma (CrI

500–604 Ma) (Figure 4), coincide with both WGD events. The additional paralog seen in *D. rerio* may be a result of the teleost-specific WGD, 450–300 Ma (Crow et al., 2006; Desvignes et al., 2021; Hoegg et al., 2004; Panopoulou & Poustka, 2005).

Our findings differ somewhat from Rytkönen et al. (2011), Graham and Presnell (2017), and Mills, Francis, Vargas, et al. (2018), which describe HIF1a and HIF2a as more closely related to each other than HIF3a. Our phylogeny (Figure 3) indicates the ancestral HIFa first duplicated to preHIF1/3 and HIF2a. In the second round, preHIF1/3 duplicated to HIF1a and HIF3a. Uncertainties in the evolutionary origin of genes that were duplicated in the vertebrate WGDs have already been observed in other proteins, for example, fibrillar collagens and lysyl oxidases (Rodriguez-Pascual & Slatter, 2016), and just like HIF, they linked intimately to oxygen metabolism (Cole et al., 2020; Mills & Canfield, 2014; Rodriguez-Pascual & Slatter, 2016). A fourth HIFa paralog (HIF4a) has been described, mostly for fishes (Graham & Presnell, 2017; Law et al., 2006; Rytkönen et al. 2008). However, given the absence of a clear phylogenetically related HIF4a group in our gene tree, it can be hypothesized the HIF4a paralog was most likely pseudogenized and then lost at some point in vertebrate evolution. Such steps are common in gene duplication events, where some duplicates may undergo neofunctionalization, subfunctionalization, or gene loss (Mighell et al., 2000; Zhang, 2003).

## 5 | CONCLUSIONS

Our results support the hypothesis of a pre-Tonian emergence of metazoans when low-oxygen conditions prevailed. The emergence of metazoan HIFa in the Mesoproterozoic Era implies that the molecular toolkit encoding hypoxia-response elements like HIF was already present in the ancestors of metazoans. We demonstrate that at least two duplication events took place along the evolutionary history of HIFa, generating HIF1a, HIF2a, and HIF3a in vertebrates. Those paralogs probably originated from the multiple rounds of genome duplications in the vertebrate stem lineage. Our study highlights the importance of molecular dating estimates of proteins as a powerful tool for understanding the evolution of these crucial ancient protein families which are intertwined with early major lineages.

### ACKNOWLEDGMENTS

This study was supported by FAPESP thematic project (Proc. 2016/06114-6), coordinated by R.I.T. A fellowship to E.M.C-P. was provided by FAPESP (Fundação de Amparo à Pesquisa do Estado de São Paulo, Brazil – Proc. 2018/20268-1). F.A.B. was funded by CNPq and FAPESP (Procs. 2019/18051-7 and 2021/14115-0). Use of SkyNet computational resources at Auburn University is acknowledged. This work was also funded in part by the National Science Foundation (grants DEB–1036537 to K.M.H. and Scott R. Santos and OCE–1155188 to K.M.H.), and FAPESP JP grant 2015/50164-5 to F.D.B.

### FUNDING INFORMATION

This study was funded by Fundação de Amparo à Pesquisa do Estado de São Paulo (FAPESP) by means of the grants: 2015/50164–5, 2016/06114–6, 2018/20268–1, 2019/18051–7 and 2021/14115–0. This study was partially funded by Conselho Nacional de Desenvolvimento Científico e Tecnológico (CNPq) grant number: 142159/2019–0. This work was also funded in part by the National Science Foundation (grants DEB–1036537 to K.M.H. and Scott R. Santos and OCE–1155188 to K.M.H.)

### CONFLICT OF INTEREST STATEMENT

The authors declare that they have no competing interests.

### DATA AVAILABILITY STATEMENT

The data that support the findings of this study are openly available within the article, its supplementary materials, and in Figshare at https://figshare.com/projects/Divergence_time_estimates_for_the_hypoxia-inducible_factor-1_alpha_HIF1_reveal_an_ancient_emergence_of_animals_in_low-oxygen_environments/164017

### ORCID

*Flavia A. Belato* https://orcid.org/0000-0003-3613-074X
*Elisa Maria Costa-Paiva* https://orcid.org/0000-0002-8470-1271

### REFERENCES

Adamska, M. (2018). Differentiation and Transdifferentiation of sponge cells. In M. Kloc & J. Kubiak (Eds.), *Marine organisms as model Systems in Biology and Medicine. Results and problems in cell differentiation* (pp. 229–253). Springer.

Alderman, S. L., Crossley, D. A., Elsey, R. M., & Gillis, T. E. (2019). Hypoxia-induced reprogramming of the cardiac phenotype in American alligators (*Alligator mississippiensis*) revealed by quantitative proteomics. *Scientific Reports*, *9*, 1–12.

Antcliffe, J. B., Callow, R. H. T., & Brasier, M. D. (2014). Giving the early fossil record of sponges a squeeze. *Biological Reviews*, *89*, 972–1004.

Bell, M. A., & Lloyd, G. T. (2015). Strap: An R package for plotting phylogenies against stratigraphy and assessing their stratigraphic congruence. *Palaeontology*, *58*, 379–389.

Benton, M., Donoghue, P., Vinther, J., Asher, R., Friedman, M., & Near, T. (2015). Constraints on the timescale of animal evolutionary history. *Palaeontologia Electronica*, *18*, 1–107.

Berná, L., & Alvarez-Valin, F. (2014). Evolutionary genomics of fast evolving tunicates. *Genome Biology and Evolution*, *6*, 1724–1738.

Bezerra, B. S., Belato, F. A., Mello, B., Brown, F., Coates, C. J., de Moraes Leme, J., Trindade, R. I. F., & Costa-Paiva, E. M. (2021). Evolution of a key enzyme of aerobic metabolism reveals Proterozoic functional subunit duplication events and an ancient origin of animals. *Scientific Reports*, *11*, 1–11.

Boden, J. S., Konhauser, K. O., Robbins, L. J., & Sánchez-Baracaldo, P. (2021). Timing the evolution of antioxidant enzymes in cyanobacteria. *Nature Communications*, *12*, 1–12.

Bouckaert, R., Heled, J., Kühnert, D., Vaughan, T., Wu, C.-H., Xie, D., Suchard, M. A., Rambaut, A., & Drummond, A. J. (2014). BEAST 2: A software platform for Bayesian evolutionary analysis. *PLoS Computational Biology*, *10*, 1–6.

Brain, C. K., Prave, A. R., Hoffmann, K.-H., Fallick, A. E., Botha, A., Herd, D. A., Sturrock, C., Young, I., Condon, D. J., & Allison, S. G. (2012). The first animals: ca. 760-million-year-old sponge-like fossils from Namibia. *South African Journal of Science*, *108*, 1–8.

Brown, C. T., Howe, A., Zhang, Q., Pyrkosz, A. B., & Brom, T. H. (2012). A reference-free algorithm for computational normalization of shotgun sequencing data. *arXiv Preprint*, 1, 1–18. bioRxiv. doi:10.48550/arXiv.1203.4802

Canfield, D. E., & Farquhar, J. (2009). Animal evolution, bioturbation, and the sulfate concentration of the oceans. *Proceedings of the National Academy of Sciences*, *106*, 8123–8127.

Canfield, D. E., Poulton, S. W., & Narbonne, G. M. (2007). Late-Neoproterozoic deep-ocean oxygenation and the rise of animal life. *Science*, *315*, 92–95.

Capella-Gutierrez, S., Silla-Martinez, J. M., & Gabaldon, T. (2009). trimAl: A tool for automated alignment trimming in large-scale phylogenetic analyses. *Bioinformatics*, *25*, 1972–1973.

Cartwright, P., & Collins, A. (2007). Fossils and phylogenies: Integrating multiple lines of evidence to investigate the origin of early major metazoan lineages. *Integrative and Comparative Biology*, *47*, 744–751.

Cole, D. B., Mills, D. B., Erwin, D. H., Sperling, E. A., Porter, S. M., Reinhard, C. T., & Planavsky, N. J. (2020). On the co-evolution of surface oxygen levels and animals. *Geobiology*, *18*, 260–281.

Costa-Paiva, E., Mello, B., Bezerra, B., Coates, C. J., Halanych, K. M., Brown, F., Leme, J., & Trindade, R. I. F. (2021). Molecular dating of the blood pigment hemocyanin provides new insight into the origin of animals. *Geobiology*, *20*, 333–345.

Crooks, G. E., Hon, G., Chandonia, J., & Brenner, S. (2004). WebLogo: A Sequence Logo Generator. *Genome Research*, *14*, 1188–1190.

Crow, K. D., Stadler, P. F., Lynch, V. J., Amemiya, C., & Wagner, G. P. (2006). The "fish-specific" hox cluster duplication is coincident with the origin of Teleosts. *Molecular Biology and Evolution*, *23*, 121–136.

Cunningham, J. A., Liu, A. G., Bengtson, S., & Donoghue, P. C. J. (2017). The origin of animals: Can molecular clocks and the fossil record be reconciled? *BioEssays*, *39*, 1–12.

Darriba, D., Taboada, G. L., Doallo, R., & Posada, D. (2011). ProtTest 3: Fast selection of best-fit models of protein evolution. *Bioinformatics*, *27*, 1164–1165.

de Mendoza, A., Sebe-Pedros, A., Sestak, M. S., Matejcic, M., Torruella, G., Domazet-Loso, T., & Ruiz-Trillo, I. (2013). Transcription factor evolution in eukaryotes and the assembly of the regulatory toolkit in multicellular lineages. *Proceedings of the National Academy of Sciences*, *110*, E4858–E4866.

Degnan, B. M., Vervoort, M., Larroux, C., & Richards, G. S. (2009). Early evolution of metazoan transcription factors. *Current Opinion in Genetics & Development*, *19*, 591–599.

Delsuc, F., Philippe, H., Tsagkogeorga, G., Simion, P., Tilak, M.-K., Turon, X., López-Legentil, S., Piette, J., Lemaire, P., & Douzery, E. J. P. (2018). A phylogenomic framework and timescale for comparative studies of tunicates. *BMC Biology*, *16*, 1–14.

Desvignes, T., Sydes, J., Montfort, J., Bobe, J., & Postlethwait, J. H. (2021). Evolution after whole-genome duplication: Teleost MicroRNAs. *Molecular Biology and Evolution*, *38*, 3308–3331.

Dohrmann, M., & Wörheide, G. (2017). Dating early animal evolution using phylogenomic data. *Scientific Reports*, *7*, 1–6.

dos Reis, M., Thawornwattana, Y., Angelis, K., Telford, M. J., Donoghue, P. C. J., & Yang, Z. (2015). Uncertainty in the timing of origin of animals and the limits of precision in molecular timescales. *Current Biology*, *25*, 2939–2950.

dos Reis, M., & Yang, Z. (2011). Approximate likelihood calculation on a phylogeny for Bayesian estimation of divergence times. *Molecular Biology and Evolution*, *28*, 2161–2172.

Douzery, E. J. P., Snell, E. A., Bapteste, E., Delsuc, F., & Philippe, H. (2004). The timing of eukaryotic evolution: Does a relaxed molecular clock reconcile proteins and fossils? *Proceedings of the National Academy of Sciences of the United States of America*, *101*, 15386–15391.

Droser, M. L., Tarhan, L. G., & Gehling, J. G. (2017). The rise of animals in a changing environment: Global ecological innovation in the late Ediacaran. *Annual Review of Earth and Planetary Sciences*, *45*, 593–617.

Drummond, A. J., Ho, S. Y. W., Phillips, M. J., & Rambaut, A. (2006). Relaxed phylogenetics and dating with confidence. *PLoS Biology*, *4*, 1–12.

Dunwoodie, S. L. (2009). The role of hypoxia in development of the mammalian embryo. *Developmental Cell*, *17*(6), 755–773.

Erwin, D. H., Laflamme, M., Tweedt, S. M., Sperling, E. A., Pisani, D., & Peterson, K. J. (2011). The Cambrian conundrum: Early divergence and later ecological success in the early history of animals. *Science*, *334*, 1091–1097.

Farquhar, J., Bao, H., & Thiemens, M. (2000). Atmospheric influence of Earth's earliest sulfur cycle. *Science*, *289*, 756–758.

Fenchel, T., & Finlay, B. J. (1995). *Ecology and evolution in anoxic worlds*. Oxford Science Publications.

Ferrario, C., Sugni, M., Somorjai, I. M. L., & Ballarin, L. (2020). Beyond adult stem cells: Dedifferentiation as a unifying mechanism underlying regeneration in invertebrate deuterostomes. *Frontiers in Cell and Developmental Biology*, *8*, 1–25.

Finn, R. D., Clements, J., & Eddy, S. R. (2011). HMMER web server: Interactive sequence similarity searching. *Nucleic Acids Research*, *39*, W29–W37.

Finn, R. D., Coggill, P., Eberhardt, R. Y., Eddy, S. R., Mistry, J., Mitchell, A. L., Potter, S. C., Punta, M., Qureshi, M., Sangrador-Vegas, A., Salazar, G. A., Tate, J., & Bateman, A. (2016). The Pfam protein families database: Towards a more sustainable future. *Nucleic Acids Research*, *44*, D279–D285.

Gene Ontology Consortium. (2004). The gene ontology (GO) database and informatics resource. *Nucleic Acids Research*, *32*, 258–261.

Glasauer, S. M. K., & Neuhauss, S. C. F. (2014). Whole-genome duplication in teleost fishes and its evolutionary consequences. *Molecular Genetics and Genomics*, *289*, 1045–1060.

Gold, D. A., & Jacobs, D. K. (2013). Stem cell dynamics in cnidaria: Are there unifying principles? *Development Genes and Evolution*, *223*, 53–66.

Grabherr, M. G., Haas, B. J., Yassour, M., Levin, J. Z., Thompson, D. A., Amit, I., Adiconis, X., Fan, L., Raychowdhury, R., Zeng, Q., Chen, Z., Mauceli, E., Hacohen, N., Gnirke, A., Rhind, N., di Palma, F., Birren, B. W., Nusbaum, C., Lindblad-Toh, K., … Regev, A. (2011). Full-length transcriptome assembly from RNA-seq data without a reference genome. *Nature Biotechnology*, *29*, 644–652.

Graham, A. M., & Presnell, J. S. (2017). Hypoxia inducible factor (HIF) transcription factor family expansion, diversification, divergence and selection in eukaryotes. *PLoS One*, *12*, 1–15.

Halanych, K. M. (2016). How our view of animal phylogeny was reshaped by molecular approaches: Lessons learned. *Organisms Diversity and Evolution*, *16*, 319–328.

Hammarlund, E. U. (2020). Harnessing hypoxia as an evolutionary driver of complex multicellularity. *Interface Focus*, *10*, 1–11.

Hammarlund, E. U., von Stedingk, K., & Påhlman, S. (2018). Refined control of cell stemness allowed animal evolution in the oxic realm. *Nature Ecology & Evolution*, *2*, 220–228.

Hedges, S. B., Blair, J. E., Venturi, M. L., & Shoe, J. L. (2004). A molecular timescale of eukaryote evolution and the rise of complex multicellular life. *BMC Evolutionary Biology*, *4*, 1–9.

Ho, S. Y. W., & Duchêne, S. (2014). Molecular-clock methods for estimating evolutionary rates and timescales. *Molecular Ecology*, *23*, 5947–5965.

Hoegg, S., Brinkmann, H., Taylor, J. S., & Meyer, A. (2004). Phylogenetic timing of the fish-specific genome duplication correlates with the diversification of teleost fish. *Journal of Molecular Evolution*, *59*, 190–203.

Hon, W. C., Wilson, M. I., Harlos, K., Claridge, T. D. W., Schofield, C. J., Pugh, C. W., Maxwell, P. H., Ratcliffe, P. J., Stuart, D. I., & Jones, E. Y. (2002). Structural basis for the recognition of hydroxyproline in HIF-1$\alpha$ by pVHL. *Nature*, *417*, 975–978.

Huerta-Cepas, J., Szklarczyk, D., Forslund, K., Cook, H., Heller, D., Walter, M. C., Rattei, T., Mende, D. R., Sunagawa, S., Kuhn, M., Jensen, L. J., von Mering, C., & Bork, P. (2016). eggNOG 4.5: A hierarchical orthology framework with improved functional annotations for eukaryotic, prokaryotic and viral sequences. *Nucleic Acids Research*, *44*, D286–D293.

Irisarri, I., Baurain, D., Brinkmann, H., Delsuc, F., Sire, J.-Y., Kupfer, A., Petersen, J., Jarek, M., Meyer, A., Vences, M., & Philippe, H. (2017). Phylotranscriptomic consolidation of the jawed vertebrate timetree. *Nature Ecology & Evolution*, *1*, 1370–1378.

Kaelin, W. G., & Ratcliffe, P. J. (2008). Oxygen sensing by metazoans: The central role of the HIF hydroxylase pathway. *Molecular Cell*, *30*, 393–402.

Kalyaanamoorthy, S., Minh, B. Q., Wong, T. K. F., von Haeseler, A., & Jermiin, L. S. (2017). ModelFinder: Fast model selection for accurate phylogenetic estimates. *Nature Methods*, *14*, 587–589.

Kanehisa, M., Goto, S., Sato, Y., Furumichi, M., & Tanabe, M. (2012). KEGG for integration and interpretation of large-scale molecular data sets. *Nucleic Acids Research*, *40*, D109–D114.

Katoh, K., & Standley, D. M. (2013). MAFFT multiple sequence alignment software version 7: Improvements in performance and usability. *Molecular Biology and Evolution*, *30*, 772–780.

Kearse, M., Moir, R., Wilson, A., Stones-Havas, S., Cheung, M., Sturrock, S., Buxton, S., Cooper, A., Markowitz, S., Duran, C., Thierer, T., Ashton, B., Meintjes, P., & Drummond, A. (2012). Geneious basic: An integrated and extendable desktop software platform for the organization and analysis of sequence data. *Bioinformatics*, *28*, 1647–1649.

King, N., & Rokas, A. (2017). Embracing uncertainty in reconstructing early animal evolution. *Current Biology*, *27*, R1081–R1088.

Kocot, K. M., Cannon, J. T., Todt, C., Citarella, M. R., Kohn, A. B., Meyer, A., Santos, S. R., Schander, C., Moroz, L. L., Lieb, B., & Halanych, K. M. (2011). Phylogenomics reveals deep molluscan relationships. *Nature*, *477*, 452–456.

Krogh, A., Larsson, B., von Heijne, G., & Sonnhammer, E. L. L. (2001). Predicting transmembrane protein topology with a hidden markov model: Application to complete genomes. *Journal of Molecular Biology*, *305*, 567–580.

Kump, L. R. (2008). The rise of atmospheric oxygen. *Nature*, *451*, 277–278.

Kuraku, S., Meyer, A., & Kuratani, S. (2008). Timing of genome duplications relative to the origin of the vertebrates: Did cyclostomes diverge before or after? *Molecular Biology and Evolution*, *26*, 47–59.

Lagesen, K., Hallin, P., Rødland, E. A., Stærfeldt, H.-H., Rognes, T., & Ussery, D. W. (2007). RNAmmer: Consistent and rapid annotation of ribosomal RNA genes. *Nucleic Acids Research*, *35*, 3100–3108.

Lartillot, N., Brinkmann, H., & Philippe, H. (2007). Suppression of long-branch attraction artefacts in the animal phylogeny using a site-heterogeneous model. *BMC Evolutionary Biology*, *7*, 1–14.

Lartillot, N., Lepage, T., & Blanquart, S. (2009). PhyloBayes 3: A Bayesian software package for phylogenetic reconstruction and molecular dating. *Bioinformatics*, *25*, 2286–2288.

Lartillot, N., & Philippe, H. (2004). A Bayesian mixture model for across-site heterogeneities in the amino-acid replacement process. *Molecular Biology and Evolution*, *21*, 1095–1109.

Law, S. H., Wu, R. S., Ng, P. K., Yu, R. M., & Kong, R. Y. (2006). Cloning and expression analysis of two distinct HIF-alpha isoforms – gcHIF-1alpha and gcHIF-4alpha – From the hypoxia-tolerant grass carp, *Ctenopharyngodon idellus*. *BMC Molecular Biology*, *7*, 1–13.

Lenton, T. M. (2020). On the use of models in understanding the rise of complex life. *Interface Focus*, *10*, 1–15.

Lenton, T. M., & Daines, S. J. (2017). Biogeochemical transformations in the history of the ocean. *Annual Review of Marine Science*, *9*, 31–58.

Lenton, T. M., & Daines, S. J. (2018). The effects of marine eukaryote evolution on phosphorus, carbon and oxygen cycling across the Proterozoic–phanerozoic transition. *Emerging Topics in Life Sciences*, *2*, 267–278.

Levin, L. A. (2003). Oxygen minimum zone benthos: Adaptation and community response to hypoxia. *Oceanography and Marine Biology: An Annual Review*, *41*, 1–45.

Li, C., Planavsky, N. J., Shi, W., Zhang, Z., Zhou, C., Cheng, M., Tarhan, L. G., Luo, G., & Xie, S. (2015). Ediacaran marine redox heterogeneity and early animal ecosystems. *Scientific Reports*, *5*, 1–8.

Liu, P., Liu, J., Ji, A., Reinhard, C. T., Planavsky, N. J., Babikov, D., Najjar, R. G., & Kasting, J. F. (2021). Triple oxygen isotope constraints on atmospheric O2 and biological productivity during the mid-Proterozoic. *Proceedings of the National Academy of Sciences*, *118*, 1–10.

Loenarz, C., Coleman, M. L., Boleininger, A., Schierwater, B., Holland, P. W. H., Ratcliffe, P. J., & Schofield, C. J. (2011). The hypoxia-inducible transcription factor pathway regulates oxygen sensing in the simplest animal, Trichoplax adhaerens. *EMBO Reports*, *12*, 63–70.

Love, G. D., Grosjean, E., Stalvies, C., Fike, D. A., Grotzinger, J. P., Bradley, A. S., Kelly, A. E., Bhatia, M., Meredith, W., Snape, C. E., Bowring, S. A., Condon, D. J., & Summons, R. E. (2009). Fossil steroids record the appearance of Demospongiae during the Cryogenian period. *Nature*, *457*, 718–721.

Lyons, T. W., Reinhard, C. T., & Planavsky, N. J. (2014). The rise of oxygen in Earth's early ocean and atmosphere. *Nature*, *506*, 307–315.

Mello, B. (2018). Estimating TimeTrees with MEGA and the TimeTree resource. *Molecular Biology and Evolution*, *35*, 2334–2342.

Mighell, A. J., Smith, N. R., Robinson, P. A., & Markham, A. F. (2000). Vertebrate pseudogenes. *FEBS Letters*, *468*, 109–114.

Mills, D. B., Boyle, R. A., Daines, S. J., Sperling, E. A., Pisani, D., Donoghue, P. C. J., & Lenton, T. M. (2022). Eukaryogenesis and oxygen in earth history. *Nature Ecology & Evolution*, *6*, 520–532.

Mills, D. B., & Canfield, D. E. (2014). Oxygen and animal evolution: Did a rise of atmospheric oxygen "trigger" the origin of animals?. *BioEssays*, *36*, 1145–1155.

Mills, D. B., Francis, W. R., & Canfield, D. E. (2018). Animal origins and the Tonian earth system. *Emerging Topics in Life Sciences*, *2*, 289–298.

Mills, D. B., Francis, W. R., Vargas, S., Larsen, M., Elemans, C. P., Canfield, D. E., & Wörheide, G. (2018). The last common ancestor of animals lacked the HIF pathway and respired in low-oxygen environments. *eLife*, *7*, 1–17.

Mills, D. B., Ward, L. M., Jones, C. A., Sweeten, B., Forth, M., Treusch, A. H., & Canfield, D. E. (2014). Oxygen requirements of the earliest animals. *Proceedings of the National Academy of Sciences of the United States of America*, *111*, 4168–4172.

Min, J.-H., Yang, H., Ivan, M., Gertler, F., Kaelin, W. G., & Pavletich, N. P. (2002). Structure of an HIF-1$\alpha$-pVHL complex: Hydroxyproline recognition in signaling. *Science*, *296*, 1886–1889.

Minh, B. Q., Nguyen, M. A. T., & von Haeseler, A. (2013). Ultrafast approximation for phylogenetic bootstrap. *Molecular Biology and Evolution*, *30*, 1188–1195.

Misof, B., Liu, S., Meusemann, K., Peters, R. S., Donath, A., Mayer, C., Frandsen, P. B., Ware, J., Flouri, T., Beutel, R. G., Niehuis, O., Petersen, M., Izquierdo-Carrasco, F., Wappler, T., Rust, J., Aberer, A. J., Aspock, U., Aspock, H., Bartel, D., … Zhou, X. (2014). Phylogenomics resolves the timing and pattern of insect evolution. *Science*, *346*, 763–767.

Mosch, T., Sommer, S., Dengler, M., Noffke, A., Bohlen, L., Pfannkuche, O., Liebetrau, V., & Wallmann, K. (2012). Factors influencing the distribution of epibenthic megafauna across the Peruvian oxygen minimum zone. *Deep Sea Research Part I: Oceanographic Research Papers*, *68*, 123–135.

Nakamura, N., Shi, X., Darabi, R., & Li, Y. (2021). Hypoxia in cell reprogramming and the epigenetic regulations. *Frontiers in Cell and Developmental Biology*, *9*, 1–10.

Narbonne, G. M. (2005). The Ediacara biota: Neoproterozoic origin of animals and their ecosystems. *Annual Review of Earth and Planetary Sciences*, *33*, 421–442.

Nguyen, L.-T., Schmidt, H. A., von Haeseler, A., & Minh, B. Q. (2015). IQ-TREE: A fast and effective stochastic algorithm for estimating

maximum-likelihood phylogenies. *Molecular Biology and Evolution*, *32*, 268–274.

Och, L. M., & Shields-Zhou, G. A. (2012). The Neoproterozoic oxygenation event: Environmental perturbations and biogeochemical cycling. *Earth-Science Reviews*, *110*, 26–57.

Panopoulou, G., & Poustka, A. J. (2005). Timing and mechanism of ancient vertebrate genome duplications - the adventure of a hypothesis. *Trends in Genetics*, *21*, 559–567.

Parfrey, L. W., Lahr, D. J. G., Knoll, A. H., & Katz, L. A. (2011). Estimating the timing of early eukaryotic diversification with multigene molecular clocks. *Proceedings of the National Academy of Sciences*, *108*, 13624–13629.

Parham, J. F., Donoghue, P. C. J., Bell, C. J., Calway, T. D., Head, J. J., Holroyd, P. A., Inoue, J. G., Irmis, R. B., Joyce, W. G., Ksepka, D. T., Patané, J. S. L., Smith, N. D., Tarver, J. E., van Tuinen, M., Yang, Z., Angielczyk, K. D., Greenwood, J. M., Hipsley, C. A., Jacobs, L., … Benton, M. J. (2012). Best practices for justifying fossil calibrations. *Systematic Biology*, *61*, 346–359.

Peet, D., & Linke, S. (2006). Regulation of HIF: Asparaginyl hydroxylation. *Novartis Foundation Symposium*, *272*, 37–49.

Petersen, T. N., Brunak, S., von Heijne, G., & Nielsen, H. (2011). SignalP 4.0: Discriminating signal peptides from transmembrane regions. *Nature Methods*, *8*, 785–786.

Peterson, K. J., Lyons, J. B., Nowak, K. S., Takacs, C. M., Wargo, M. J., & McPeek, M. A. (2004). Estimating metazoan divergence times with a molecular clock. *Proceedings of the National Academy of Sciences*, *101*, 6536–6541.

Pisani, D., Pett, W., Dohrmann, M., Feuda, R., Rota-Stabelli, O., Philippe, H., Lartillot, N., & Wörheide, G. (2015). Genomic data do not support comb jellies as the sister group to all other animals. *Proceedings of the National Academy of Sciences*, *112*, 15402–15407.

Pu, J. P., Bowring, S. A., Ramezani, J., Myrow, P., Raub, T. D., Landing, E., Mills, A., Hodgin, E., & Macdonald, F. A. (2016). Dodging snowballs: Geochronology of the Gaskiers glaciation and the first appearance of the Ediacaran biota. *Geology*, *44*, 955–958.

Purcell, J. E., Breitburg, D. L., Decker, M. B., Graham, W. M., Youngbluth, M. J., & Raskoff, K. A. (2001). Pelagic cnidarians and ctenophores in low dissolved oxygen environments: A review. In N. N. Rabalais & R. E. Turner (Eds.), *Coastal hypoxia: Consequences for living resources and ecosystems* (pp. 77–100). American Geophyical Union.

Rambaut, A. (2009). FigTree: Tree Figure Drawing Tool. Version 1.2.2. http://tree.bio.ed.ac.uk/software/figtree/

Rambaut, A., Suchard, M. A., Xie, D., & Drummond, A. J. (2015). Tracer. Version 1.6. http://beast.community/tracer

Reinhard, C. T., Planavsky, N. J., Olson, S. L., Lyons, T. W., & Erwin, D. H. (2016). Earth's oxygen cycle and the evolution of animal life. *Proceedings of the National Academy of Sciences*, *113*, 8933–8938.

Rodriguez-Pascual, F., & Slatter, D. A. (2016). Collagen cross-linking: Insights on the evolution of metazoan extracellular matrix. *Scientific Reports*, *6*, 1–7.

Ronquist, F., & Huelsenbeck, J. P. (2003). MrBayes 3: Bayesian phylogenetic inference under mixed models. *Bioinformatics*, *19*, 1572–1574.

Rytkönen, K. T., Ryynänen, H. J., Nikinmaa, M., & Primmer, C. R. (2008). Variable patterns in the molecular evolution of the hypoxia-inducible factor-1 alpha (HIF-1$\alpha$) gene in teleost fishes and mammals. *Gene*, *420*, 1–10.

Rytkönen, K. T., Williams, T. A., Renshaw, G. M., Primmer, C. R., & Nikinmaa, M. (2011). Molecular evolution of the metazoan PHD-HIF oxygen-sensing system. *Molecular Biology and Evolution*, *28*, 1913–1926.

Sacerdot, C., Louis, A., Bon, C., Berthelot, C., & Roest Crollius, H. (2018). Chromosome evolution at the origin of the ancestral vertebrate genome. *Genome Biology*, *19*, 1–15.

Sahoo, S. K., Planavsky, N. J., Kendall, B., Wang, X., Shi, X., Scott, C., Anbar, A. D., Lyons, T. W., & Jiang, G. (2012). Ocean oxygenation in the wake of the Marinoan glaciation. *Nature*, *489*, 546–549.

Sebé-Pedrós, A., de Mendoza, A., Lang, B. F., Degnan, B. M., & Ruiz-Trillo, I. (2011). Unexpected repertoire of metazoan transcription factors in the unicellular holozoan *Capsaspora owczarzaki*. *Molecular Biology and Evolution*, *28*, 1241–1254.

Sebé-Pedrós, A., Zheng, Y., Ruiz-Trillo, I., & Pan, D. (2012). Premetazoan origin of the hippo signaling pathway. *Cell Reports*, *1*, 13–20.

Semenza, G. L. (2007). Life with oxygen. *Science*, *318*, 62–64.

Shih, P. M., & Matzke, N. J. (2013). Primary endosymbiosis events date to the later Proterozoic with cross-calibrated phylogenetic dating of duplicated ATPase proteins. *Proceedings of the National Academy of Sciences of the United States of America*, *110*, 12355–12360.

Simakov, O., Marlétaz, F., Yue, J.-X., O'Connell, B., Jenkins, J., Brandt, A., Calef, R., Tung, C.-H., Huang, T.-K., Schmutz, J., Satoh, N., Yu, J.-K., Putnam, N. H., Green, R. E., & Rokhsar, D. S. (2020). Deeply conserved synteny resolves early events in vertebrate evolution. *Nature Ecology & Evolution*, *4*, 820–830.

Simionato, E., Ledent, V., Richards, G., Thomas-Chollier, M., Kerner, P., Coornaert, D., Degnan, B. M., & Vervoort, M. (2007). Origin and diversification of the basic helix-loop-helix gene family in metazoans: Insights from comparative genomics. *BMC Evolutionary Biology*, *7*, 1–18.

Simon, M. C., & Keith, B. (2008). The role of oxygen availability in embryonic development and stem cell function. *Nature Reviews Molecular Cell Biology*, *9*, 285–296.

Song, H., Chen, X., Jiao, Q., Qiu, Z., Shen, C., Zhang, G., Sun, Z., Zhang, H., & Luo, Q.-Y. (2021). HIF-1$\alpha$-mediated telomerase reverse transcriptase activation inducing autophagy through mammalian target of rapamycin promotes papillary thyroid carcinoma progression during hypoxia stress. *Thyroid*, *31*, 233–246.

Sperling, E. A., Frieder, C. A., Raman, A. V., Girguis, P. R., Levin, L. A., & Knoll, A. H. (2013). Oxygen, ecology, and the Cambrian radiation of animals. *Proceedings of the National Academy of Sciences of the United States of America*, *110*, 13446–13451.

Sperling, E. A., Knoll, A. H., & Girguis, P. R. (2015). The ecological physiology of Earth's second oxygen revolution. *Annual Review of Ecology, Evolution, and Systematics*, *46*, 215–235.

Suga, H., Chen, Z., de Mendoza, A., Sebé-Pedrós, A., Brown, M. W., Kramer, E., Carr, M., Kerner, P., Vervoort, M., Sánchez-Pons, N., Torruella, G., Derelle, R., Manning, G., Lang, B. F., Russ, C., Haas, B. J., Roger, A. J., Nusbaum, C., & Ruiz-Trillo, I. (2013). The Capsaspora genome reveals a complex unicellular prehistory of animals. *Nature Communications*, *4*, 1–9.

Tarade, D., Lee, J. E., & Ohh, M. (2019). Evolution of metazoan oxygen-sensing involved a conserved divergence of VHL affinity for HIF1$\alpha$ and HIF2$\alpha$. *Nature Communications*, *10*, 1–12.

Taylor, C. T., & McElwain, J. C. (2010). Ancient atmospheres and the evolution of oxygen sensing via the hypoxia-inducible factor in metazoans. *Physiology*, *25*, 272–279.

Thuesen, E. V., Rutherford, L. D., & Brommer, P. L. (2005). The role of aerobic metabolism and intragel oxygen in hypoxia tolerance of three ctenophores: *Pleurobrachia bachei*, *Bolinopsis infundibulum* and *Mnemiopsis leidyi*. *Journal of the Marine Biological Association of the United Kingdom*, *85*, 627–633.

Tostevin, R., & Mills, B. J. W. (2020). Reconciling proxy records and models of Earth's oxygenation during the Neoproterozoic and Palaeozoic: Neoproterozoic-Palaeozoic oxygenation. *Interface Focus*, *10*, 1–13.

Tsagkogeorga, G., Cahais, V., & Galtier, N. (2012). The population genomics of a fast evolver: High levels of diversity, functional constraint, and molecular adaptation in the tunicate Ciona intestinalis. *Genome Biology and Evolution*, *4*, 852–861.

Tsagkogeorga, G., Turon, X., Hopcroft, R. R., Tilak, M.-K., Feldstein, T., Shenkar, N., Loya, Y., Huchon, D., Douzery, E. J., & Delsuc, F. (2009). An updated 18S rRNA phylogeny of tunicates based on mixture and secondary structure models. *BMC Evolutionary Biology*, *9*, 1–16.

Tsuji, K., Kitamura, S., & Makino, H. (2014). Hypoxia-inducible factor 1$\alpha$ regulates branching morphogenesis during kidney development. *Biochemical and Biophysical Research Communications*, *447*, 108–114.

Turner, E. C. (2021). Possible poriferan body fossils in early Neoproterozoic microbial reefs. *Nature*, *596*, 87–91.

Wang, Y., Shi, S., Liu, H., & Meng, L. (2016). Hypoxia enhances direct reprogramming of mouse fibroblasts to cardiomyocyte-like cells. *Cellular Reprogramming*, *18*, 1–7.

Weigert, A., Helm, C., Meyer, M., Nickel, B., Arendt, D., Hausdorf, B., Santos, S. R., Halanych, K. M., Purschke, G., Bleidorn, C., & Struck, T. H. (2014). Illuminating the base of the annelid tree using transcriptomics. *Molecular Biology and Evolution*, *31*, 1391–1401.

Weits, D. A., Kunkowska, A. B., Kamps, N. C. W., Portz, K. M. S., Packbier, N. K., Nemec Venza, Z., Gaillochet, C., Lohmann, J. U., Pedersen, O., van Dongen, J. T., & Licausi, F. (2019). An apical hypoxic niche sets the pace of shoot meristem activity. *Nature*, *569*, 714–717.

Whelan, N., Kocot, K. M., Moroz, L. L., & Halanych, K. M. (2015). Error, signal, and the placement of Ctenophora sister to all other animals. *Proceedings of the National Academy of Sciences*, *112*, 5773–5778.

Whelan, S., & Goldman, N. (2001). A general empirical model of protein evolution derived from multiple protein families using a maximum-likelihood approach. *Molecular Biology and Evolution*, *18*, 691–699.

Wolfe, J. M., Breinholt, J. W., Crandall, K. A., Lemmon, A. R., Lemmon, E. M., Timm, L. E., Siddall, M. E., & Bracken-Grissom, H. D. (2019). A phylogenomic framework, evolutionary timeline and genomic resources for comparative studies of decapod crustaceans. *Proceedings of the Royal Society B: Biological Sciences*, *286*, 1–10.

Wood, R., Liu, A. G., Bowyer, F., Wilby, P. R., Dunn, F. S., Kenchington, C. G., Cuthill, J. F. H., Mitchell, E. G., & Penny, A. (2019). Integrated records of environmental change and evolution challenge the Cambrian explosion. *Nature Ecology and Evolution*, *3*, 528–538.

Yang, Z. (2007). PAML 4: Phylogenetic analysis by maximum likelihood. *Molecular Biology and Evolution*, *24*, 1586–1591.

Yin, Z., Zhu, M., Davidson, E. H., Bottjer, D. J., Zhao, F., & Tafforeau, P. (2015). Sponge grade body fossil with cellular resolution dating 60 Myr before the Cambrian. *Proceedings of the National Academy of Sciences*, *112*, E1453–E1460.

Young, M. D., Wakefield, M. J., Smyth, G. K., & Oshlack, A. (2010). Gene ontology analysis for RNA-seq: Accounting for selection bias. *Genome Biology*, *11*, 1–12.

Yu, H., & Li, L. (2014). Phylogeny and molecular dating of the cerato-platanin-encoding genes. *Genetics and Molecular Biology*, *37*, 423–427.

Zhang, F., Xiao, S., Kendall, B., Romaniello, S. J., Cui, H., Meyer, M., Gilleaudeau, G. J., Kaufman, A. J., & Anbar, A. D. (2018). Extensive marine anoxia during the terminal Ediacaran period. *Science Advances*, *4*, 1–11.

Zhang, J. (2003). Evolution by gene duplication: An update. *Trends in Ecology & Evolution*, *18*, 292–298.

## SUPPORTING INFORMATION

Additional supporting information can be found online in the Supporting Information section at the end of this article.

**How to cite this article:** Belato, F. A., Mello, B., Coates, C. J., Halanych, K. M., Brown, F. D., Morandini, A. C., de Moraes Leme, J., Trindade, R. I. F., & Costa-Paiva, E. M. (2024). Divergence time estimates for the hypoxia-inducible factor-1 alpha (HIF1α) reveal an ancient emergence of animals in low-oxygen environments. *Geobiology*, *22*, e12577. https://doi.org/10.1111/gbi.12577